

24433

IMAGE IDENTIFICATION AND RESTORATION  
USING EM ALGORITHM

by

Yücel Yemez

B.S. in E.E., Middle East Technical University, 1989

Submitted to the Institute for Graduate Studies in  
Science and Engineering in partial fulfillment of

the requirements for the degree of

Master of Science

in

Electrical Engineering

Boğaziçi University

1992

**IMAGE IDENTIFICATION AND RESTORATION  
USING EM ALGORITHM**

**APPROVED BY**

Doç. Dr. Emin Anarım

.....  
Emin Anarım

(Thesis Supervisor)

Prof. Dr. Yorgo İstefanopulos

.....  
Yorgo İstefanopulos

(Thesis Co-supervisor)

Y. Doç. Dr. Aysın Ertüzün

.....  
Aysın Ertüzün

Doç. Dr. Ahmet Kayran

.....  
Ahmet Kayran

**DATE OF APPROVAL**

## ACKNOWLEDGEMENTS

I would like to express my thanks to

Assoc. Prof. Emin Anarım and Prof. Yorgo İstefanopulos for their valuable help and guidance throughout the study,

Assist. Prof. Aysin Ertüzün and Assoc. Prof. Ahmet Kayran for having participated as committee members in my presentation,

Alp Öztarhan for his valuable help in computer programming.

## ABSTRACT

This thesis considers the problem of identification and restoration of images degraded by additive Gaussian white noise. It is assumed that the power of the noise and the statistical properties of the original image are not known a priori. A new approach which reduces the two dimensional problem to a one dimensional problem by using the unitary discrete Fourier transform is introduced. Then, by applying the expectation-maximization (EM) algorithm, the image is restored and the parameters of various types of AR models are identified under noisy conditions. Two different methods are used for restoration, namely, maximum likelihood restoration and Kalman filtering. The simulation results of the presented approach are also included.

## ÖZET

Bu çalışmada toplamsal Gauss dağılımlı beyaz gürültü ile bozulmuş imgelerin tanınması ve onarımı sorunu ele alınmıştır. Gürültünün gücünün ve imgenin istatistiksel özelliklerinin önceden bilinmediği varsayılmıştır. İki boyutlu sorunu, ayrık Fourier dönüşümünü kullanarak tek boyuta indiren yeni bir yaklaşım tanıtılmış ve daha sonra beklenti-embüytme (EM) algoritması uygulanarak, imge gürültülü ortamlarda onarılmış ve değişik özbağlanımlı (AR) modellerin parametreleri bulunmuştur. İmge onarımı için, Kalman süzmesi ve embüyük olabilirlik onarımı olmak üzere, iki farklı yöntem kullanılmıştır. Tanıtılan yaklaşımın benzetim sonuçları da çalışmaya eklenmiştir.

## TABLE OF CONTENTS

<b>ACKNOWLEDGEMENTS</b>	<b>iii</b>
<b>ABSTRACT</b>	<b>iv</b>
<b>ÖZET</b>	<b>v</b>
<b>LIST OF FIGURES</b>	<b>viii</b>
<b>LIST OF TABLES</b>	<b>x</b>
<b>LIST OF SYMBOLS</b>	<b>xi</b>
<b>LIST OF ABBREVIATIONS</b>	<b>xiii</b>
<b>I INTRODUCTION</b>	<b>1</b>
1.1 Statement of the Problem . . . . .	1
1.2 The Scope of the Thesis . . . . .	2
<b>II STOCHASTIC IMAGE MODELLING</b>	<b>4</b>
2.1 2-D AR Modelling . . . . .	4
2.2 Model Fitting . . . . .	7
2.2.1 Least Squares Method . . . . .	7
2.2.2 Stability of 2-D AR Models . . . . .	8
<b>III IDENTIFICATION AND RESTORATION</b>	
<b>USING EM ALGORITHM</b>	<b>9</b>
3.1 Overview of Stochastic Image Restoration . . . . .	9
3.1.1 Bayesian Estimator . . . . .	9

3.1.2	Wiener Filtering . . . . .	10
3.1.3	Kalman Filtering . . . . .	10
3.2	Maximum Likelihood Identification and Restoration . . . . .	11
3.3	EM Algorithm . . . . .	13
3.3.1	The E-step of the Algorithm . . . . .	14
3.3.2	The M-step of the Algorithm . . . . .	15
3.3.3	Discussion . . . . .	15
<b>IV</b>	<b>REDUCTION OF DIMENSIONALITY</b>	<b>16</b>
4.1	Image Model . . . . .	16
4.2	Diagonalization of the Coefficient Matrices . . . . .	18
4.2.1	Diagonalization with DST . . . . .	19
4.2.2	Diagonalization with DFT . . . . .	20
4.3	Decomposition into Scalar Subsystems . . . . .	21
4.4	EM Algorithm . . . . .	24
4.4.1	E-step (Restoration) . . . . .	24
4.4.2	M-step (Identification) . . . . .	26
4.5	Identification of the 2-D AR Parameters . . . . .	29
4.6	Summary . . . . .	31
4.7	Experimental Results . . . . .	32
4.8	Discussion . . . . .	45
4.9	Comments on Further Research . . . . .	47
<b>V</b>	<b>CONCLUSION</b>	<b>49</b>
	<b>APPENDIX A</b>	<b>51</b>
	<b>APPENDIX B</b>	<b>52</b>
	<b>APPENDIX C</b>	<b>54</b>

## LIST OF FIGURES

1	Examples of some commonly used model supports for various first order AR models . . . . .	5
2	Structure of EM Algorithm . . . . .	13
3	Schematic representation of the identification and restoration algorithm . . . . .	31
4	The original face image . . . . .	36
5	0 dB noisy image . . . . .	36
6	The image restored in DFT domain against 0 dB noise by Kalman filtering. . . . .	37
7	The image restored in DST domain against 0 dB noise by Kalman filtering . . . . .	37
8	The image restored in DFT domain against 0 dB noise by maximum likelihood approach. . . . .	38
9	The image restored in DST domain against 0 dB noise by maximum likelihood approach . . . . .	38
10	5 dB noisy image . . . . .	39



11	The image restored in DFT domain against 5 dB noise by Kalman filtering. . . . .	40
12	The image restored in DST domain against 5 dB noise by Kalman filtering. . . . .	40
13	The image restored in DFT domain against 5 dB noise by maximum likelihood approach. . . . .	41
14	The image restored in DST domain against 5 dB noise by maximum likelihood approach. . . . .	41
15	10 dB noisy image . . . . .	42
16	The image restored in DFT domain against 10 dB noise by Kalman filtering. . . . .	43
17	The image restored in DST domain against 10 dB noise by Kalman filtering . . . . .	43
18	The image restored in DFT domain against 10 dB noise by maximum likelihood approach. . . . .	44
19	The image restored in DST domain against 10 dB noise by maximum likelihood approach. . . . .	44

## LIST OF TABLES

1	Performance of restoration in DFT domain . . . . .	34
2	Performance of restoration in DST domain . . . . .	34
3	The results of identification by DFT . . . . .	35
4	The results of identification by DST . . . . .	35




## LIST OF SYMBOLS

$\mathbf{A}$	Image model matrix of size $N^2 \times N^2$
$\mathbf{A}_k$	Image model matrix of size $N \times N$
$a(k, l)$	Image model coefficients
$\mathbf{F}$	Defining matrix of DFT
$f_k(W_N^j)$	$j$ th entry of the diagonalized form of the $k$ th image model coefficient matrix.
$\mathcal{L}(\theta)$	Log-likelihood function
$\mathbf{P}$	Conditional covariance matrix of the original image with size $N^2 \times N^2$
$\mathbf{Q}_v$	Covariance matrix of the observation noise with size $N^2 \times N^2$
$\mathbf{Q}_w$	Covariance matrix of the model noise with size $N^2 \times N^2$
$S$	Image model support
$\mathbf{T}$	Defining matrix of DST
$\mathbf{v}$	Observation noise
$\mathbf{w}$	Model noise
$\mathbf{x}$	Original image
$\hat{\mathbf{x}}$	Restored or estimated image

$y$	Observed image
$z$	DFT of the original image
$\zeta$	DFT of the observation noise
$\eta$	DFT of the observed image
$\Theta$	A priori unknown parameters
$\xi$	DFT of the model noise
$\rho$	Signal to noise ratio
$\sigma_v^2$	Variance of the observation noise
$\sigma_w^2$	Variance of the model noise
$\sigma_\zeta^2$	Variance of the transformed observation noise
$\sigma_\xi^2$	Variance of the transformed model noise

## LIST OF ABBREVIATIONS

AR	Autoregressive
DFT	Discrete Fourier transform
DST	Discrete Sine transform
EM	Expectation-Maximization
LS	Least squares
pdf	Probability density function
PSF	Point spread function



# I INTRODUCTION

## 1.1 Statement of the Problem

Restoration of images can be defined as the general problem of estimating a two dimensional (2-D) object from a degraded version of this object. The cause of these degradations are generally the imperfections in the electronic or photographic medium. Blurring and noise are two important and dominant types of degradation. Blurring can be introduced by relative motion between camera and the original scene, by an optical system which is out of focus, or atmospheric turbulence. On the other hand, noise may be caused by the transmission medium, the recording medium, inaccurate measurement or, quantization of the data for digital storage.

An image is generally defined as a real or complex valued function of two space variables belonging to some support region. Although this support may be continuous, it is commonly sampled on a rectangular grid. This defines a set of pixels and the image can be represented by an array  $x(n, m)$  of pixel intensity levels. In this thesis, we deal with monochromatic images of pixels representing the gray levels, degraded by an additive Gaussian white noise with zero mean. We assume that there is no blurring or another type of noise —like multiplicative noise— in the observed image and try to recover the original image from its observed version degraded by the additive Gaussian white noise. Therefore, the degradation can be modelled as,

$$y(n, m) = x(n, m) + v(n, m) \quad (1)$$

where  $y(n, m)$  denotes the observed image and  $v(n, m)$  represents the zero-mean Gaussian white observation noise with variance  $\sigma_v^2$ .

*Restoration of images requires some statistical knowledge of both the original image  $x(n, m)$  and the observation noise  $v(n, m)$ . Therefore, restoration can be re-defined as estimating  $x(n, m)$  given the observed image  $y(n, m)$  and some statistical knowledge of  $x(n, m)$  and  $v(n, m)$ . Image identification concerns with estimating this knowledge prior to the restoration.* However, it should be pointed out that image identification and image restoration are *separate* problems and the use of image identification is *not* limited to only image restoration. The mentioned statistical knowledge of the image is also useful in several other fields of image processing, e.g., image data compression, coding, filtering and image analysis [1].

## 1.2 The Scope of the Thesis

This thesis addresses the problem of image identification and restoration when the observation noise is not known *a priori* and concentrates on the reduction of dimensionality.

Chapter II studies the 2-D stochastic modelling for image processing and forms the mathematical groundwork for the study of image identification and restoration. In this chapter we briefly review the 2-D autoregressive (AR) image models and the use of the well known least squares (LS) method in the realization of these models.

Chapter III begins with a review of classical stochastic image restoration methods and discusses some shortcomings of these methods. In the rest of the chapter, we summarize the image identification and restoration method using expectation-

maximization (EM) algorithm, which has been developed by Lagendijk [2].

Chapter IV concentrates on reduction of dimensionality. Since images are generally 2-D objects, image processing methods are usually 2-D. In this chapter we develop an algorithm which decomposes the image into scalar subsystems and which, in this way, reduces the problem of image identification and restoration to a 1-D problem. Our method is similar to the method developed by Katayama [3]. The advantage of our algorithm is that it is capable to identify the parameters of various 2-D AR models. In this chapter, we also use the restoration method developed by Lagendijk [2] more efficiently. At the end of the chapter, we display the experimental results of the algorithm and compare with the results in [3].

Finally, in chapter V, we make concluding remarks on this thesis study.



## II STOCHASTIC IMAGE MODELLING

Restoration of images requires a priori statistical knowledge of the original image  $x(n, m)$  and the observation noise  $v(n, m)$ . This statistical knowledge is the the concern of image identification. However, soon a new question comes into the mind: What is the type of this statistical knowledge? In order to answer this question, we have to develop a mathematical model for the original image.

### 2.1 2-D AR Modelling

The development of a suitable mathematical model for an image requires a trade off between its accuracy of representation and its utility for the application. In view of the experimental results obtained by many researchers, we use the following 2-D autoregressive (AR) model driven by a zero mean random noise,

$$x(n, m) = \sum_{k, l \in S} a(k, l)x(n - k, m - l) + w(n, m) \quad (2)$$

where  $a(k, l)$  denotes the image model coefficients which are determined by minimizing the variance of the noise  $\sigma_w^2 = E[w^2(n, m)]$ . Here  $E[.]$  denotes the mathematical expectation. Therefore,  $w(n, m)$  can be considered as the modelling noise.

In (2),  $S$  stands for the image model support. Some common model supports for various first order AR models are shown in Figure 1.

2-D AR models are useful in many fields of image processing like image data transmission and storage via DPCM coding, hybrid coding, design of recursive,

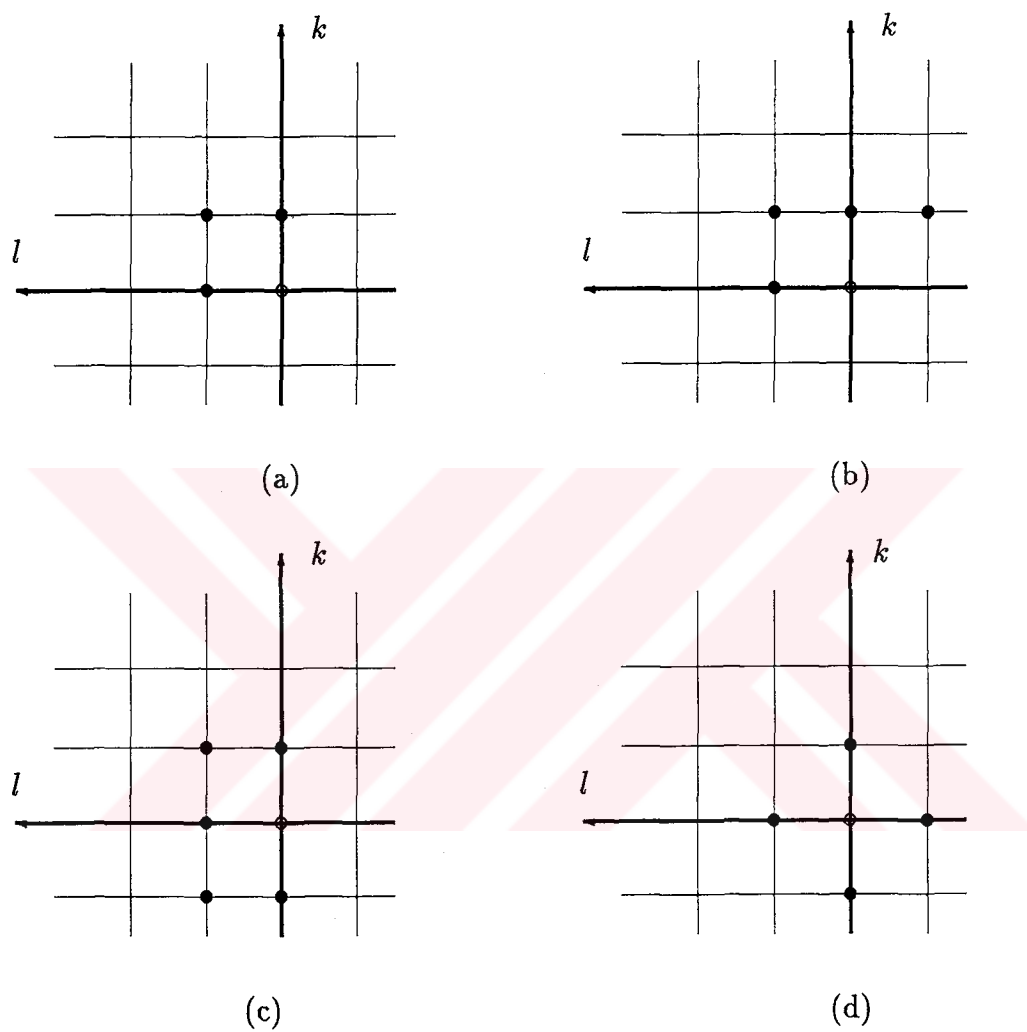


Figure 1: Examples of some commonly used model supports for various first order AR models, (a) quarter plane causal, (b) nonsymmetric halfplane causal, (c) semi-causal, (d) noncausal.

semirecursive and nonrecursive filters for image estimation, restoration and filtering and image analysis [1].

Although *the choice of the model support depends on the application*, nonsymmetric halfplane (NSHP) model support has various advantages over the others, as becomes apparent, e.g. in 2-D Kalman filtering [4, 5] and the factorization of 2-D spectra [6]. Further, the NSHP<sup>1</sup> image model immediately allows for a 2-D recursion without the necessity to delay the observations.

An alternative compact notation of (2) and (1) is,

$$\mathbf{x} = \mathbf{A}\mathbf{x} + \mathbf{w} \quad (3)$$

$$\mathbf{y} = \mathbf{x} + \mathbf{v} \quad (4)$$

where  $\mathbf{x}$ ,  $\mathbf{y}$ ,  $\mathbf{w}$  and  $\mathbf{v}$  are the lexicographically<sup>2</sup> ordered vectors of size  $N^2 \times 1$  for  $x(n, m)$ ,  $y(n, m)$ ,  $w(n, m)$  and  $v(n, m)$  respectively.  $\mathbf{A}$  is the AR model coefficient matrix of size  $N^2 \times N^2$ . If the boundary problem is solved by assuming that the image is circulant, then  $\mathbf{A}$  has a block circulant structure.

We will denote the covariance matrices of  $\mathbf{w}$  and  $\mathbf{v}$  by  $\mathbf{Q}_w$  and  $\mathbf{Q}_v$  of size  $N^2 \times N^2$ , respectively. Since we assume that observation noise is white, we can write the covariance of  $\mathbf{v}$  as,

$$\mathbf{Q}_v = \sigma_v^2 \mathbf{I} \quad (5)$$

---

<sup>1</sup>We note that in 2-D literature, the term 'causal' is often used for only quarter plane models. In this thesis, we regard NSHP model as causal.

<sup>2</sup>Lexicographically ordering means to scan the 2-D data row by row and stack into a vector.

## 2.2 Model Fitting

Since the image model (2) is completely determined by the model coefficient matrix  $\mathbf{A}$  and the model noise covariance matrix  $\mathbf{Q}_w$ , the a priori knowledge of the original image which image identification concerns with, is the knowledge of  $\mathbf{A}$  and  $\mathbf{Q}_w$ .

### 2.2.1 Least Squares Method

The entries of the model coefficient matrix  $\mathbf{A}$  are the model coefficients  $a(k, l)$  in (2). Therefore, the problem of image model identification is generally defined to be minimizing the variance of the model noise

$$\sigma_w^2 = \frac{1}{N^2} \sum_{n=1, m=1}^N \left( x(n, m) - \sum_{k, l \in S} a(k, l) x(n - k, m - l) \right)^2 \quad (6)$$

with respect to  $a(k, l)$  if the image is assumed to be of size  $N \times N$ .

If  $\mathbf{a}$  denotes the coefficient matrix and  $\mathbf{x}_1(n - 1, m)$  denotes the vector formed by the pixel values  $x(n - k, m - l)$  in the model support of  $x(n, m)$ , (6) can be rewritten in vector form as,

$$\sigma_w^2 = \frac{1}{N^2} \sum_{n=1, m=1}^N \left( x(n, m) - \mathbf{a}^t \mathbf{x}_1(n - 1, m) \right)^2$$

Setting to zero the gradient of  $\sigma_w^2$  with respect to  $\mathbf{a}$  yields

$$\hat{\mathbf{a}} = \left[ \sum_{n, m \in W} \mathbf{x}_1(n - 1, m) \mathbf{x}_1^t(n - 1, m) \right]^{-1} \left[ \sum_{n, m \in W} \mathbf{x}_1(n - 1, m) x(n, m) \right]$$

This is a straightforward procedure if we do not worry about the observation noise. For noisy images, this method, which is referred to as least squares method,

has been modified in [5]. The modified method uses directly the noisy observation and is called as bias-compensated least squares method. However, the method assumes that the noise is known *a priori* and makes some expectation approximations which yield poor performance at high noise levels [5].

### 2.2.2 Stability of 2-D AR Models

2-D AR models can only be useful in designing image processing techniques, if the underlying model is BIBO (bounded-input, bounded-output) stable. Otherwise, small errors in calculations can cause large errors in the result [1].

Identification of image models by minimizing the variance of the model noise does not necessarily lead to stable models or does not assure that the resulting noise is white. This is the case for semicausal and noncausal AR models. Therefore, the model noise in (2) is not necessarily a white noise process since we assume the model as minimum variance representation model (MVR)<sup>3</sup> [1].

In the case of causal models, fortunately, if we fit a model by minimizing the variance of the modelling noise, the resulting model is assured to be stable and white noise driven [1].

---

<sup>3</sup>In AR modelling, there are two important types of noise modelling: white noise driven representation (WNR) and minimum variance representation (MVR).

## III IDENTIFICATION AND RESTORATION USING EM ALGORITHM

Classical approaches in the field of image identification and restoration assume that the observation noise is known *a priori*, i.e, identification and restoration are possible only if this assumption is valid. With this assumption, a suitable model is found for the original image and then the restoration is performed. In recent studies of Lagendijk [2] and Katayama [3], methods which do not assume that the observation noise is known *a priori*, and which perform the identification and restoration concurrently have been developed. These methods use the well known EM (Expectation-Maximization) algorithm and maximum likelihood approach.

### 3.1 Overview of Stochastic Image Restoration

Before going into EM Algorithm, in this section we briefly summarize three classical stochastic image restoration methods. We exclude non-stochastic approaches like iterative and algebraic restoration [8, 9].

#### 3.1.1 Bayesian Estimator

With the assumption that the original image and the observation noise are Gaussian with zero mean, the Bayesian estimator of the original image  $\mathbf{x}$  maximizes the a posteriori probability density function (pdf)  $p(\mathbf{x} | \mathbf{y})$  with respect to  $\mathbf{x}$  and

yields the following restoration equation [2],

$$\hat{\mathbf{x}} = (\mathbf{I} + \mathbf{R}_{vv}\mathbf{R}_{xx}^{-1})^{-1}\mathbf{y}$$

where  $\mathbf{R}_{vv}$  and  $\mathbf{R}_{xx}$  denote the correlation matrices of  $\mathbf{v}$  and  $\mathbf{x}$ , respectively. Therefore, Bayesian estimator requires some a priori knowledge of the original image and the observation noise.

### 3.1.2 Wiener Filtering

The Wiener filter is designed to minimize the mean squared error between the original image  $\mathbf{x}$  and the restoration result  $\hat{\mathbf{x}}$ . The solution to this rather classical problem is given by [7, 2],

$$\hat{\mathbf{x}} = (\mathbf{I} + \mathbf{R}_{vv}\mathbf{R}_{xx}^{-1})^{-1}\mathbf{y}$$

which is identical to the Bayesian estimator under the Gaussian assumptions. The correlation matrix  $\mathbf{R}_{xx}$  is usually approximated using the observed image. Although the method may work satisfactorily at low noise levels, its performance becomes poor when the noise level is high.

### 3.1.3 Kalman Filtering

Direct application of classical 1-D Kalman filtering to the problem of 2-D filtering results in a very large state vector and therefore, excessive computation. To overcome this excessive computational load, a 2-D version of Kalman filter has been adapted [4, 10]. The method is known as reduced update Kalman filtering (RUKF).

Like Wiener filtering, Kalman filtering aims to minimize the mean squared error between the original and the restored image. Here, we do not go into the details of this well known filtering. This method also requires the a priori knowledge of the observation noise and makes use of the NSHP AR modelling (Figure 1). Moreover, the method is suboptimal since reduction of the state vector means an approximation to the optimal solution.

### 3.2 Maximum Likelihood Identification and Restoration

Maximum likelihood approach requires the definition and optimization of a likelihood function for the image.

Image identification aims to determine the unknown parameters of the image, which we denote by  $\Theta$ . In our case,  $\Theta$  includes the model coefficients  $a(k, l)$ , the variance of the model noise  $\sigma_w^2$  and the variance of the observation noise  $\sigma_v^2$ , i.e., the parameter vector  $\Theta$  can be written as

$$\Theta = [a(k, l), \sigma_w^2, \sigma_v^2]$$

With this definition of  $\Theta$ , the likelihood function is given by

$$p(\mathbf{x}, \mathbf{y} | \Theta) = p(\mathbf{y} | \mathbf{x}, \Theta)p(\mathbf{x} | \Theta) \quad (7)$$

where the conditional pdf of  $\mathbf{x}$  given  $\Theta$  is

$$p(\mathbf{x} | \Theta) = \prod_{n=1, m=1}^N (2\pi\sigma_w^2)^{-1/2} \exp \left\{ -\frac{1}{2\sigma_w^2} \sum_{n=1, m=1}^N \left( x(n, m) - \sum_{k, l \in S} a(k, l)x(n-k, m-l) \right)^2 \right\} \quad (8)$$



and the conditional pdf of  $\mathbf{y}$  given  $\mathbf{x}, \Theta$  is

$$p(\mathbf{y} | \mathbf{x}, \Theta) = \prod_{n=1, m=1}^N (2\pi\sigma_v^2)^{-1/2} \exp \left\{ -\frac{1}{2\sigma_v^2} \sum_{n=1, m=1}^N (y(n, m) - x(n, m))^2 \right\} \quad (9)$$

In writing (8) and (9), we assume that the modelling noise  $\mathbf{w}$  is a Gaussian white random process as well as the observation noise. (Therefore, 2-D AR modelling is necessarily causal). Using (8) and (9), the log-likelihood function is given by

$$\begin{aligned} \mathcal{L}(\Theta) &= -\log p(\mathbf{x}, \mathbf{y} | \Theta) \\ &= \frac{N^2}{2} \log 2\pi + \frac{N^2}{2} \log \sigma_w^2 + \frac{1}{2\sigma_w^2} \sum_{n=1, m=1}^N \left( x(n, m) - \sum_{k, l \in S} a(k, l) x(n-k, m-l) \right)^2 \\ &\quad + \frac{N^2}{2} \log 2\pi + \frac{N^2}{2} \log \sigma_v^2 + \frac{1}{2\sigma_v^2} \sum_{n=1, m=1}^N (y(n, m) - x(n, m))^2 \end{aligned} \quad (10)$$

In view of (7) and (10), we state:

- Image identification problem is to find the best estimate for  $\Theta$  which maximizes the likelihood function (7) or equivalently the log-likelihood function (10), given the original image  $\mathbf{x}$  and the observed image  $\mathbf{y}$ .
- Image restoration problem is to find the best estimate for  $\mathbf{x}$ , which also maximizes (10), given  $\mathbf{y}$  and the parameters  $\Theta$ .

At first sight, these two statements seem to make no sense since we assume that  $\Theta$  and  $\mathbf{x}$  are not known a priori. However, the use of EM algorithm makes these statements rather meaningful.

### 3.3 EM Algorithm

It has been shown that EM-like algorithms lead to computationally efficient estimation algorithms in various signal processing applications [11, 12].

EM algorithm has two steps: Expectation (E-step) and Maximization (M-step). Algorithm starts with some initial parameters  $\Theta_0$ . In E-step, using  $\Theta_0$  and the observed image  $\mathbf{y}$ , the image is restored maximizing (10). In M-step, using the restored image  $\hat{\mathbf{x}}$ ,  $\Theta$  is updated again by maximizing (10). Then, we return to E-step and restore the image, this time using the updated parameters  $\hat{\Theta}$ . The algorithm continues so on until  $\hat{\Theta}$  converges. (See Figure 2)

In EM Algorithm, M-step corresponds to identification of the unknown parameters maximizing the likelihood function. That is why we call this step as *maximization step*. On the other hand, E-step corresponds to restoration of the original image. Maximization of the likelihood function with respect to  $\mathbf{x}$  is equivalent to finding the expected value of  $\mathbf{x}$  using its conditional pdf which is given

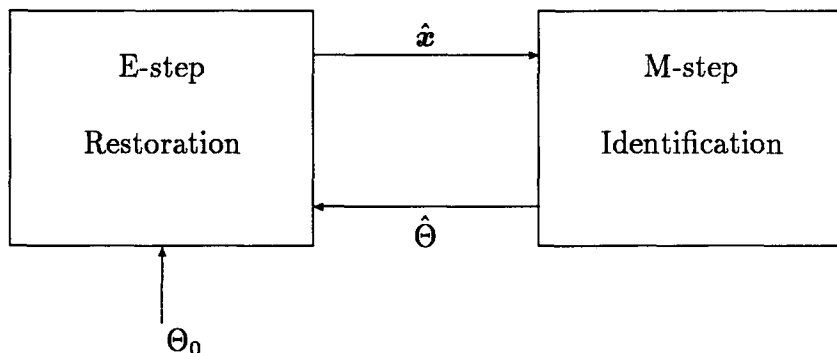


Figure 2: Structure of EM Algorithm

by

$$p(\mathbf{x} | \mathbf{y}, \Theta) = \frac{p(\mathbf{x}, \mathbf{y} | \Theta)}{p(\mathbf{y} | \Theta)}$$

since finding the expected value of a random variable is equivalent to maximization of its pdf<sup>4</sup>. That is why we call this step as *expectation* step.

Under the conditions that  $\sigma_w^2 > 0$ ,  $\sigma_v^2 > 0$  and that  $(\mathbf{I} - \mathbf{A})$  is nonsingular, EM algorithm is assured to converge [2, 13]. However, a critical problem is choosing  $\Theta_0$ , the initial value of  $\Theta$ , since  $\Theta$  may converge to a local optimum of the likelihood function rather than the global optimum.

### 3.3.1 The E-Step of the Algorithm

A more compact expression for  $p(\mathbf{x}, \mathbf{y} | \Theta)$  might be written in vector form as

$$p(\mathbf{x}, \mathbf{y} | \Theta) = \sqrt{\frac{\det|\mathbf{I} - \mathbf{A}|^2}{2\pi^{2N^2} \det|\mathbf{Q}_v \mathbf{Q}_w|}} \exp \left\{ -\frac{1}{2}(\mathbf{y} - \mathbf{x})^t \mathbf{Q}_v^{-1}(\mathbf{y} - \mathbf{x}) - \frac{1}{2}\mathbf{x}^t(\mathbf{I} - \mathbf{A})\mathbf{x} \right\}$$

where  $\mathbf{Q}_v$  and  $\mathbf{Q}_w$  are covariance matrices of  $\mathbf{v}$  and  $\mathbf{w}$  with size  $N^2 \times N^2$ , respectively and given by

$$\mathbf{Q}_w = \sigma_w^2 \mathbf{I} \quad (11)$$

$$\mathbf{Q}_v = \sigma_v^2 \mathbf{I} \quad (12)$$

Maximizing  $p(\mathbf{x}, \mathbf{y} | \Theta)$  with respect to  $\mathbf{x}$  or equivalently, taking the expectation of  $\mathbf{x}$  with respect to  $p(\mathbf{x} | \mathbf{y}, \Theta)$  yields the following restoration equation[2]:

$$\hat{\mathbf{x}} = \mathbb{E}(\mathbf{x} | \mathbf{y}, \Theta) = \hat{\mathbf{P}}\mathbf{Q}_w^{-1}\mathbf{y} \quad (13)$$

---

<sup>4</sup>Observe that  $p(\mathbf{y} | \Theta)$  is not a function of  $\mathbf{x}$ .

where  $\hat{\mathbf{P}}$  denotes the covariance matrix of  $\mathbf{x}$ , which is given by

$$\hat{\mathbf{P}} = \text{Cov}(\mathbf{x} \mid \mathbf{y}, \Theta) = \left[ (\mathbf{I} - \mathbf{A})^t \mathbf{Q}_v^{-1} (\mathbf{I} - \mathbf{A}) + \mathbf{Q}_w^{-1} \right]^{-1} \quad (14)$$

### 3.3.2 The M-step of the Algorithm

If we assume that we have the original image restored in E-step, the identification problem becomes similar to the least squares method described in Section 2.2.1. However, for an accurate identification we should take into account that the restored image  $\hat{\mathbf{x}}$  is not identical to the original image  $\mathbf{x}$ , but its optimum estimate. Therefore, in M-step we make use of the correlation matrix of  $\mathbf{x}$  which is given by

$$\hat{\mathbf{R}}_{xx} = \text{E}(\mathbf{x}\mathbf{x}^t \mid \mathbf{y}, \Theta) = \hat{\mathbf{P}} + \hat{\mathbf{x}}\hat{\mathbf{x}}^t \quad (15)$$

Further details for the M-step will be considered in the next chapter.

### 3.3.3 Discussion

An important disadvantage of this application of EM algorithm is the computational load caused by the operations on large matrices, e.g. in the restoration equation (13) we have to operate on matrices with size  $N^2 \times N^2$ . In the next chapter, we will discuss some ways to reduce this computational load.

Another disadvantage is that it is applicable only to causal image models. We recall that one necessary condition for EM Algorithm to be assured to converge is the requirement for the matrix  $(\mathbf{I} - \mathbf{A})$  to be nonsingular. In case the modelling is causal,  $(\mathbf{I} - \mathbf{A})$  is a lower triangular matrix and therefore,  $\det(\mathbf{I} - \mathbf{A}) = 1$  which means that it is nonsingular. However, when the modelling is semicausal or noncausal,  $(\mathbf{I} - \mathbf{A})$  is not necessarily nonsingular.

## IV REDUCTION OF DIMENSIONALITY

Since images are generally 2-D objects, most of the classical methods in image processing require 2-D filtering. However, 2-D processing of images yields computationally more complex algorithms when compared to 1-D signal processing. This fact becomes apparent in for instance 2-D Kalman filtering. When we implement Kalman filtering in 2-D, we encounter the problem of enormously large state vector when compared to 1-D Kalman filtering and a computationally feasible filtering becomes possible only if we make some approximations on the size of the state vector. With this motivation, in this chapter we will discuss the problem of reduction of dimensionality for image identification and restoration. We will consider only the first order AR models to simplify the notation.

### 4.1 Image Model

We recall the 2-D AR modelling (2) and define the following vectors,

$$\mathbf{x}(m) = [x(1, m), \dots, x(N, m)]^t$$

$$\mathbf{w}(m) = [w(1, m), \dots, w(N, m)]^t$$

$$\mathbf{y}(m) = [y(1, m), \dots, y(N, m)]^t$$

$$\mathbf{v}(m) = [v(1, m), \dots, v(N, m)]^t$$

Then, considering only the first order models, (2) and (1) become

$$\mathbf{A}_0 \mathbf{x}(m) = \mathbf{A}_1 \mathbf{x}(m-1) + \mathbf{w}(m) \tag{16}$$

$$\mathbf{y}(m) = \mathbf{x}(m) + \mathbf{v}(m) \tag{17}$$

where  $\mathbf{A}_0$  and  $\mathbf{A}_1$  are coefficient matrices determined by the 2-D AR model coefficients  $a(k, l)$ . For all types of AR models (causal, semicausal or noncausal), the coefficient matrices are circulant if we solve the boundary problem by assuming the image is circulant.

We note that for noncausal AR modelling, (16) has an additional coefficient matrix  $\mathbf{A}_{-1}$ . Therefore, in our derivation we will exclude the noncausal AR modelling. However, since  $\mathbf{A}_{-1}$  is also circulant, it is also possible to modify the algorithm and extend it to noncausal AR models.

Below, we list the first rows of the circulant coefficient matrices for various first order AR models:

1. Quarterplane causal AR model:

$$\mathbf{A}_0 \rightarrow [1 \ 0 \ \cdots \ 0 \ -a_{10}]$$

$$\mathbf{A}_1 \rightarrow [a_{01} \ 0 \ \cdots \ 0 \ a_{11}]$$

2. NSHP causal AR model:

$$\mathbf{A}_0 \rightarrow [1 \ 0 \ \cdots \ 0 \ -a_{10}]$$

$$\mathbf{A}_1 \rightarrow [a_{01} \ a_{-1,1} \ 0 \ \cdots \ 0 \ a_{11}]$$

3. Symmetric-semicausal<sup>5</sup> AR model:

$$\mathbf{A}_0 \rightarrow [1 \ -a_{10} \ 0 \ \cdots \ 0 \ -a_{10}]$$

$$\mathbf{A}_1 \rightarrow [a_{01} \ a_{11} \ 0 \ \cdots \ 0 \ a_{11}]$$

4. Symmetric-noncausal AR model:

$$\mathbf{A}_0 \rightarrow [1 \ -a_{10} \ 0 \ \cdots \ 0 \ -a_{10}]$$

$$\mathbf{A}_1 \rightarrow [a_{01} \ 0 \ \cdots \ 0]$$

$$\mathbf{A}_{-1} \rightarrow [a_{0,-1} \ 0 \ \cdots \ 0]$$

---

<sup>5</sup>Symmetric modelling implies  $a_{kl} = a_{-k,l}$

Therefore, the coefficient matrices are all circulant with the first rows given above. We note that the coefficient matrices for the symmetric semicausal model are also symmetric banded Toeplitz matrices.

Since the model noise of causal models is white, the covariance of  $\mathbf{w}(m)$  in (16) can be written as

$$\mathbb{E}[\mathbf{w}(m)\mathbf{w}^t(m)] = \sigma_w^2 \mathbf{I} \quad (18)$$

For symmetric semicausal models, it is possible to assume the covariance as [3, 14]

$$\mathbb{E}[\mathbf{w}(m)\mathbf{w}^t(m)] = \sigma_w^2 \mathbf{A}_0 \mathbf{I} \quad (19)$$

Since the modelling is symmetric, the covariance matrix in (19) is assured to be symmetric. As for the covariance of the uncorrelated observation noise  $\mathbf{v}(m)$ :

$$\mathbb{E}[\mathbf{v}(m)\mathbf{v}^t(m)] = \sigma_v^2 \mathbf{I} \quad (20)$$

and the cross covariance of  $\mathbf{w}(m)$  and  $\mathbf{v}(m)$  is

$$\mathbb{E}[\mathbf{v}(m)\mathbf{w}^t(m)] = 0 \quad (21)$$

## 4.2 Diagonalization of the Coefficient Matrices

Unitary transforms are useful in many fields of image processing. Two important unitary transforms are discrete Fourier transform (DFT) and discrete sine transform (DST).

### 4.2.1 Diagonalization with DST

The idea of reducing the dimension by using unitary DST belongs to Jain [14]. According to his factorization result [15], the coefficient matrices  $\mathbf{A}_0$  and  $\mathbf{A}_1$  of the *symmetric semicausal* AR model can be almost diagonalized by DST, i.e.

$$\mathbf{T}\mathbf{A}_k\mathbf{T} \cong \mathbf{\Lambda}$$

where  $\mathbf{\Lambda}$  is a diagonal matrix and  $\mathbf{T}$  is the defining matrix of DST which is given by

$$\mathbf{T} = \left\{ \sqrt{\frac{2}{N+1}} \sin \frac{nm\pi}{N+1} \right\}, \quad 1 \leq n, m \leq N$$

This result is the consequence of the fact that any  $N \times N$  real, symmetric banded Toeplitz matrix  $\mathbf{A}$  can be factored as

$$\mathbf{A} = \mathbf{A}_p + \mathbf{A}_b$$

$\mathbf{A}_b$  is a Hankel matrix and  $\mathbf{A}_p$  is a  $p$ th order polynomial in a symmetric, tridiagonal matrix.

DST diagonalizes  $\mathbf{A}_p$ . Therefore, when we neglect the matrix  $\mathbf{A}_b$ , we can say that DST diagonalizes  $\mathbf{A}$ . Actually, this is a valid approximation. For example, when the AR model is of first order, the coefficient matrices in (16) are completely diagonalized. When the order increases, the effects of  $\mathbf{A}_b$  comes into the picture. Therefore, for a reasonable value of the order  $p$  which should be sufficiently small as compared with  $N$ , we can say that DST almost diagonalizes the coefficient matrices.



### 4.2.2 Diagonalization with DFT

Including the symmetric semicausal model, all types of AR models yield circulant coefficient matrices (see Section 4.1). Any circulant matrix can be diagonalized by unitary DFT [7], therefore

$$\mathbf{F} \mathbf{A}_k \mathbf{F}^* = \text{diag}(f_k(W_N^0), f_k(W_N^1), \dots, f_k(W_N^{N-1})) \quad (22)$$

where  $\mathbf{A}_k$  denotes the coefficient matrices and  $\mathbf{F}$  is the defining matrix of DFT, which is given by

$$\mathbf{F} = \left\{ \frac{1}{\sqrt{N}} W_N^{jn} \right\}, \quad 0 \leq j, n \leq N-1$$

where by definition

$$W_N = \exp \frac{-i2\pi}{N} \quad (23)$$

In (22), the diagonal elements denote the eigenvalues of the coefficient matrix  $\mathbf{A}_k$  and are given by the DFT of its first column:

$$f_k(W_N^j) = \sum_{l=0}^{N-1} h_k(l) W_N^{jl}, \quad 0 \leq j \leq N-1 \quad (24)$$

where  $\{h_k(l)\}$  denotes the first column of the coefficient matrix  $\mathbf{A}_k$ . Recalling that DST almost diagonalizes the coefficient matrices of the symmetric semicausal AR model, we note that when we use DFT, we do not have to make any approximation on the diagonalization of the coefficient matrices.

### 4.3 Decomposition into Scalar Subsystems

In this section, using the diagonalization results of the previous section, we aim to decompose the 2-D image into 1-D scalar subsystems to which we will apply the EM algorithm for image identification and restoration. A similar method has already been developed by Katayama [3], using DST, so which is applicable only when the modelling is symmetric semicausal. What we will do in the rest of this chapter is to generalize his method to various 2-D AR models. Therefore, we will derive the algorithm once more, this time using DFT. Throughout the derivation, for the sake of notational simplicity, we will consider the first order AR models. It is also possible to extend the derivation to higher order AR models.

We define the DFT's of the vectors of (16) and (17) as

$$\begin{aligned} \mathbf{z}(m) &= \mathbf{F}\mathbf{x}(m) & \boldsymbol{\xi}(m) &= \mathbf{F}\mathbf{A}_0^{-1}\mathbf{w}(m) \\ \boldsymbol{\eta}(m) &= \mathbf{F}\mathbf{y}(m) & \boldsymbol{\zeta}(m) &= \mathbf{F}\mathbf{v}(m) \end{aligned} \quad (25)$$

and taking the DFT of (16) and (17) yields (see Appendix A)

$$\begin{aligned} \mathbf{F}\mathbf{x}(m) &= \boldsymbol{\Lambda}\mathbf{F}\mathbf{x}(m-1) + \mathbf{F}\mathbf{A}_0^{-1}\mathbf{w}(m) \\ \mathbf{F}\mathbf{y}(m) &= \mathbf{F}\mathbf{x}(m) + \mathbf{F}\mathbf{v}(m) \end{aligned} \quad (26)$$

where

$$\boldsymbol{\Lambda} = \text{diag}\left(f_0^{-1}(W_N^0)f_1(W_N^0), \dots, f_0^{-1}(W_N^{N-1})f_1(W_N^{N-1})\right) \quad (27)$$

and it follows,

$$\begin{aligned} \mathbf{z}(m) &= \boldsymbol{\Lambda}\mathbf{z}(m-1) + \boldsymbol{\xi}(m) \\ \boldsymbol{\eta}(m) &= \mathbf{z}(m) + \boldsymbol{\zeta}(m) \end{aligned} \quad (28)$$

Using (27), (28) can be written in scalar notation as

$$z_j(m) = a_j z_j(m-1) + \xi_j(m) \quad (29)$$

$$\eta_j(m) = z_j(m) + \zeta_j(m) \quad (30)$$

where the subscript  $j$  denotes the  $j$  th elements of the vectors in (25) and

$$a_j = \frac{f_1(W_N^j)}{f_0(W_N^j)} \quad (31)$$

We note that the scalars in (29) and (30) are all complex valued. Therefore, although the modelling equations of each subsystem seem to be the same with the ones that Katayama has obtained in his work, the problem is different.

Since DFT is a unitary transform and since total energy is conserved in unitary transforms, we can write the covariances of the transformed complex scalars  $\xi_j(m)$  and  $\zeta_j(m)$  as (see Appendix B),

$$E[\xi_j(m)\xi_l^*(k)] = \frac{\sigma_w^2}{|f_0(W_N^j)|^2} \delta_{jl} \delta_{mk} \quad (32)$$

$$E[\zeta_j(m)\zeta_l^*(k)] = \sigma_v^2 \delta_{jl} \delta_{mk} \quad (33)$$

$$E[\xi_j(m)\zeta_l^*(k)] = 0$$

(32) is valid for causal AR models. For symmetric semicausal modelling, we can write

$$E[\xi_j(m)\xi_l^*(k)] = \frac{\sigma_w^2}{|f_0(W_N^j)|^2} \delta_{jl} \delta_{mk} \quad (34)$$

We see that  $\xi_j(m)$  and  $\xi_l(m)$  are uncorrelated for  $j \neq l$  and so are  $\zeta_j(m)$  and  $\zeta_l(m)$ .

Omitting the subscript  $j$ , we rewrite (29) and (30) as

$$z(m) = az(m-1) + \xi(m) \quad (35)$$

$$\eta(m) = z(m) + \zeta(m) \quad (36)$$

Writing the imaginary and real parts of complex scalars, we get

$$\begin{aligned} z_r(m) &= a_r z_r(m-1) - a_i z_i(m-1) + \xi_r(m) \\ z_i(m) &= a_i z_r(m-1) + a_r z_i(m-1) + \xi_i(m) \end{aligned} \quad (37)$$

$$\begin{aligned} \eta_r(m) &= z_r(m) + \zeta_r(m) \\ \eta_i(m) &= z_i(m) + \zeta_i(m) \end{aligned} \quad (38)$$

where the subscripts  $i$  and  $r$  denote the imaginary and the real parts, respectively.

A deeper analysis (see Appendix C) and experimental experience show that the imaginary and the real parts of  $\mathbf{z}(m)$  are uncorrelated so that

$$a_i = 0 \quad (39)$$

Therefore, (37) and (38) can be rewritten as

$$\begin{aligned} z_r(m) &= a z_r(m-1) + \xi_r(m) \\ \eta_r(m) &= z_r(m) + \zeta_r(m) \end{aligned} \quad (40)$$

$$\begin{aligned} z_i(m) &= a z_i(m-1) + \xi_i(m) \\ \eta_i(m) &= z_i(m) + \zeta_i(m) \end{aligned} \quad (41)$$

where  $a$  is a real scalar.

The real and the imaginary parts of DFT are actually two separate linear transformations. Since the linear transformation of a Gaussian random process yields a Gaussian random process [16], by equations (32), (33), (40) and (41) we get

$$\begin{aligned} \mathbb{E}[\boldsymbol{\xi}_r(m) \boldsymbol{\xi}_r^t(k)] &= \sigma_{\xi_r}^2 \mathbf{I} \delta_{mk} \\ \mathbb{E}[\boldsymbol{\zeta}_r(m) \boldsymbol{\zeta}_r^t(k)] &= \sigma_{\zeta_r}^2 \mathbf{I} \delta_{mk} \end{aligned} \quad (42)$$

$$\begin{aligned}
\mathbb{E}[\boldsymbol{\xi}_i(m)\boldsymbol{\xi}_i^t(k)] &= \sigma_{\xi_i}^2 \mathbf{I} \delta_{mk} \\
\mathbb{E}[\boldsymbol{\zeta}_i(m)\boldsymbol{\zeta}_i^t(k)] &= \sigma_{\zeta_i}^2 \mathbf{I} \delta_{mk}
\end{aligned} \tag{43}$$

Therefore,  $\boldsymbol{\xi}_r(m)$ ,  $\boldsymbol{\xi}_i(m)$ ,  $\boldsymbol{\zeta}_r(m)$  and  $\boldsymbol{\zeta}_i(m)$  are Gaussian uncorrelated (white) random processes with zero mean.

## 4.4 EM Algorithm

By the equations (40), (41), (42) and (43), we have now  $2N$  independent 1-D scalar subsystems in the transform domain. We will apply the EM Algorithm to each of the subsystems and restore the real and the imaginary parts of the DFT image row by row.

### 4.4.1 E-step (Restoration)

Assuming that we know the parameters  $\Theta$  identified by the M-step, we restore the transformed image using two different approaches: Maximum likelihood restoration and Kalman filtering.

#### Maximum Likelihood Restoration

Recalling the restoration equations (13) and (14) of Section 3.3.1, first we write (40) and (41), in matrix form as

$$\begin{aligned}
\mathbf{z}_r &= \mathbf{a}\mathbf{z}_r + \boldsymbol{\xi}_r \\
\boldsymbol{\eta}_r &= \mathbf{z}_r + \boldsymbol{\zeta}_r
\end{aligned} \tag{44}$$

$$\begin{aligned} \mathbf{z}_i &= \mathbf{a}\mathbf{z}_i + \boldsymbol{\xi}_i \\ \boldsymbol{\eta}_i &= \mathbf{z}_i + \boldsymbol{\zeta}_i \end{aligned} \quad (45)$$

Since the real and the imaginary parts are independent of each other, we can restore  $\mathbf{z}_r$  and  $\mathbf{z}_i$  separately. Using (13) and (14), we get the following restoration equations for the real part,

$$\hat{\mathbf{z}}_r = \mathbb{E}(\mathbf{z}_r | \boldsymbol{\eta}_r, \Theta) = \hat{\mathbf{P}}_r \mathbf{Q}_{\zeta_r}^{-1} \boldsymbol{\eta}_r \quad (46)$$

$$\hat{\mathbf{P}}_r = \text{Cov}(\mathbf{z}_r | \boldsymbol{\eta}_r, \Theta) = [(\mathbf{I} - \mathbf{a})^t \mathbf{Q}_{\xi_r}^{-1} (\mathbf{I} - \mathbf{a}) + \mathbf{Q}_{\zeta_r}^{-1}]^{-1} \quad (47)$$

where  $\mathbf{Q}_{\xi_r}$  and  $\mathbf{Q}_{\zeta_r}$  are the covariance matrices of  $\boldsymbol{\xi}_r$  and  $\boldsymbol{\zeta}_r$ , respectively and are given by

$$\mathbf{Q}_{\xi_r} = \sigma_{\xi_r}^2 \mathbf{I}$$

$$\mathbf{Q}_{\zeta_r} = \sigma_{\zeta_r}^2 \mathbf{I}$$

Restoration equations for the imaginary part is identical to those for the real part except for a subscript  $i$  instead of  $r$ . However, we note that  $\sigma_{\xi_i}^2$  and  $\sigma_{\xi_r}^2$  are not necessarily the same and are identified by the M-step and so are  $\sigma_{\zeta_i}^2$  and  $\sigma_{\zeta_r}^2$ . In (46) and (47),  $\Theta$  denotes the parameters  $a, \sigma_{\xi_i}^2, \sigma_{\xi_r}^2, \sigma_{\zeta_r}^2$  and  $\sigma_{\zeta_i}^2$ . Coefficient matrix  $\mathbf{a}$  is a  $N \times N$  circulant matrix with the first row

$$[0 \cdots 0 \ a]$$

When we recall (13) and (14) in Section 3.3.1 by which the image is restored without decomposition, we observe that we have to deal with matrices of size  $N^2 \times N^2$  in order to get the restored image. On the other hand, the restoration equations (46) and (47) which we get by decomposition require operations on matrices of size  $N \times N$ . Therefore, the computational load of the maximum likelihood restoration algorithm decreases significantly.

## 1-D Kalman Filtering

The significance in reduction of the computational load by decomposition becomes much more apparent if we see that the equations (40) and (41) are suitable forms for applying 1-D Kalman filter and the fixed interval smoother [17, 18]. Therefore, what we do in order to restore the image is just to apply 1-D Kalman filter and backward smoother to the rows of the DFT image modelled by (40) and (41). 1-D Kalman filtering followed by a smoother is computationally much more efficient when compared to maximum likelihood restoration.

### 4.4.2 M-step (Identification)

If the system parameters are not known *a priori*, which is our case, we have to identify these parameters from  $\boldsymbol{\eta}$  prior to restoration. System parameters are identified by maximizing the likelihood function  $p(\mathbf{z}_r, \mathbf{z}_i, \boldsymbol{\eta}_r, \boldsymbol{\eta}_i \mid \Theta_r, \Theta_i)$ . In view of the equations (10), (40) and (41), the log-likelihood function can be written as (omitting the constant terms)

$$\begin{aligned}
 \mathcal{L}(\Theta_r, \Theta_i) &= \frac{N}{2} \log \sigma_{\xi_r}^2 + \frac{1}{2\sigma_{\xi_r}^2} \sum_{m=1}^N (z_r(m) - az_r(m-1))^2 + \\
 &\quad \frac{N}{2} \log \sigma_{\xi_i}^2 + \frac{1}{2\sigma_{\xi_i}^2} \sum_{m=1}^N (z_i(m) - az_i(m-1))^2 + \\
 &\quad \frac{N}{2} \log \sigma_{\zeta_r}^2 + \frac{1}{2\sigma_{\zeta_r}^2} \sum_{m=1}^N (\eta_r(m) - z_r(m))^2 + \\
 &\quad \frac{N}{2} \log \sigma_{\zeta_i}^2 + \frac{1}{2\sigma_{\zeta_i}^2} \sum_{m=1}^N (\eta_i(m) - z_i(m))^2 \tag{48}
 \end{aligned}$$

Partially differentiating  $\mathcal{L}(\Theta_r, \Theta_i)$  with respect to  $a, \sigma_{\xi_r}^2, \sigma_{\xi_i}^2, \sigma_{\zeta_r}^2, \sigma_{\zeta_i}^2$  and setting the derivatives to zero so as to maximize the log-likelihood function yields the

following update equations for the unknown parameters

$$\begin{aligned}
\hat{a} &= \frac{\sum z_r(m)z_r(m-1) + z_i(m)z_i(m-1)}{\sum z_r^2(m-1) + z_i^2(m-1)} \\
\hat{\sigma}_{\xi_r}^2 &= \frac{1}{N} \sum (z_r(m) - az_r(m-1))^2 \\
\hat{\sigma}_{\xi_i}^2 &= \frac{1}{N} \sum (z_i(m) - az_i(m-1))^2 \\
\hat{\sigma}_{\zeta_r}^2 &= \frac{1}{N} \sum (\eta_r(m) - z_r(m))^2 \\
\hat{\sigma}_{\zeta_i}^2 &= \frac{1}{N} \sum (\eta_i(m) - z_i(m))^2
\end{aligned} \tag{49}$$

for  $m = 1, \dots, N$ .

As the output of the restoration in the E-step, we get the expected values  $\hat{z}_r$  and  $\hat{z}_i$ , not the true values of  $z_r$  and  $z_i$ . Therefore, recalling the correlation equation (15) and using the covariance matrices ( or equivalently, the error covariances ) which can be found by (47) or by the Kalman filter and the smoother, we can rewrite the update equations (49) in terms of  $\hat{z}_r(m)$  and  $\hat{z}_i(m)$  as

$$\begin{aligned}
\hat{a} &= \frac{\sum \hat{z}_r(m)\hat{z}_r(m-1) + P_r(m, m-1 | N) + \hat{z}_i(m)\hat{z}_i(m-1) + P_i(m, m-1 | N)}{\sum \hat{z}_r^2(m-1) + P_r(m-1 | N) + \hat{z}_i^2(m-1) + P_i(m-1 | N)} \\
\hat{\sigma}_{\xi_r}^2 &= \frac{1}{N} \sum \hat{z}_r^2(m) + P_r(m | N) - 2a\hat{z}_r(m)\hat{z}_r(m-1) - 2aP_r(m, m-1 | N) \\
&\quad + a^2\hat{z}_r^2(m-1) + a^2P_r(m-1 | N) \\
\hat{\sigma}_{\zeta_r}^2 &= \frac{1}{N} \sum \eta_r^2(m) - 2\eta_r(m)\hat{z}_r(m) + \hat{z}_r^2(m) + P(m | N)
\end{aligned} \tag{50}$$

where  $P_r(m | N)$  and  $P_r(m, m-1 | N)$  denote the error covariances.

The update of the variances  $\hat{\sigma}_{\xi_i}^2$  and  $\hat{\sigma}_{\zeta_i}^2$  are identical to the update of the variances of the real part in terms of  $P_i(m | N)$ ,  $P_i(m, m-1 | N)$  and  $\hat{z}_i(m)$ .

Update equations (50) supply the necessary system parameters for the E-step.



By iterating the computation of the expectation for  $\mathbf{z}_r$  and  $\mathbf{z}_i$  and the update of the parameters, we obtain the parameters for each row ( $j = 0, \dots, N - 1$ ) of the DFT image. At this point, we are to make the following remarks:

1. Since the 1-D AR modelling which we use for the transformed DFT image is causal,  $(\mathbf{I} - \mathbf{a})$  is a lower triangular matrix and nonsingular. Moreover,  $\hat{\sigma}_{\xi_r}^2, \hat{\sigma}_{\xi_i}^2, \hat{\sigma}_{\zeta_r}^2$  and  $\hat{\sigma}_{\zeta_i}^2$  are positive. Therefore, EM Algorithm is assured to converge.
2. If  $\sigma_\xi^2$  and  $\sigma_\zeta^2$  denote the variances of the complex modelling noise and observation noise in (35) and (36), then by (37) and (38) we get

$$\begin{aligned}\sigma_\xi^2 &= \text{E}[\xi(m)\xi^*(m)] = \sigma_{\xi_r}^2 + \sigma_{\xi_i}^2 \\ \sigma_\zeta^2 &= \text{E}[\zeta(m)\zeta^*(m)] = \sigma_{\zeta_r}^2 + \sigma_{\zeta_i}^2\end{aligned}\quad (51)$$

and by (32) and (33)

$$\begin{aligned}\sigma_w^2 &= |f_0(W_N^j)|^2 (\sigma_{\xi_r}^2(j) + \sigma_{\xi_i}^2(j)) \\ \sigma_v^2 &= \sigma_\zeta^2(j)\end{aligned}\quad (52)$$

for  $j = 0, \dots, N - 1$ .

3. 1-D AR models for  $\mathbf{z}_r$  and  $\mathbf{z}_i$  in (40) and (41) are not necessarily minimum variance models as also seen in the update equation (50) for  $a$ , i.e the updated parameter  $\hat{a}$  does not necessarily make the variances  $\sigma_{\xi_r}^2$  and  $\sigma_{\xi_i}^2$  minimum. However, recalling (35) and (36), we see that  $\sigma_\xi^2$  given by (51) is minimized. (40) and (41) are actually white noise driven models, i.e.  $\xi_r$  and  $\xi_i$  are Gaussian white random processes.

## 4.5 Identification of the 2-D AR Parameters

The output of the EM algorithm is the restored image and the identified parameters in the transform domain. Original image can easily be restored by taking the inverse DFT of the estimated image.

In this section, we derive an identification algorithm that determines the parameters of the original 2-D AR model based on the AR parameters of the DFT image. The method makes use of the well known least squares method and is similar to the algorithm in [3].

While the algorithm in [3] is capable to identify only the 2-D symmetric semi-causal AR parameters, our identification algorithm can be used to identify any kind of 2-D AR (causal or semicausal ) model parameters since we have not assumed any specific AR modelling in the derivation of the EM algorithm.

We derive the identification algorithm for only the quarter plane causal model (see Figure 1). However, it can easily be generalized to the other AR models.

Recalling the coefficient matrices  $\mathbf{A}_0$  and  $\mathbf{A}_1$  in Section 4.1 for the first order quarter-plane causal model and using (24) , we write

$$\begin{aligned} f_0(W_N^j) &= 1 - a_{10}W_N^j \\ f_1(W_N^j) &= a_{01} + a_{11}W_N^j \end{aligned} \quad (53)$$

where  $a_{01}$ ,  $a_{10}$  and  $a_{11}$  are the AR parameters of the original image model.

Using (31) and (53) we get

$$a_j = \frac{a_{01} + a_{11}(\cos \frac{2\pi}{N}j + i \sin \frac{2\pi}{N}j)}{1 - a_{10}(\cos \frac{2\pi}{N}j + i \sin \frac{2\pi}{N}j)}, \quad j = 0, \dots, N - 1 \quad (54)$$

where  $a_j$  is the AR coefficient of the  $j$ th row of the DFT image.

(54) yields two equations for the real and the imaginary part:

$$\begin{aligned} a_{01} + a_{10}a_j \cos \frac{2\pi}{N}j + a_{11} \cos \frac{2\pi}{N}j &= a_j \\ a_{10}a_j \sin \frac{2\pi}{N}j + a_{11} \sin \frac{2\pi}{N}j &= 0 \end{aligned} \quad (55)$$

for  $j = 0, \dots, N - 1$ .

(55) is a system of  $2N$  linear equations with 3 unknowns. Therefore, we can write (55) in matrix form as

$$\mathbf{B}\mathbf{a} = \mathbf{b} \quad (56)$$

where  $\mathbf{B}$  is of size  $2N \times 3$ ,  $\mathbf{b}$  is of size  $2N \times 1$  and  $\mathbf{a}$  is a  $3 \times 1$  matrix formed by the 2-D AR coefficients.

Solution of (56) is given by the least squares method:

$$\mathbf{a} = (\mathbf{B}^t\mathbf{B})^{-1}\mathbf{B}^t\mathbf{b} \quad (57)$$

where  $\mathbf{B}^t\mathbf{B}$  is a matrix with size  $3 \times 3$ .

Solving (57) is equivalent to find the parameters  $a_{01}$ ,  $a_{10}$  and  $a_{11}$  which fit best to the equation (56).

It is also possible to estimate the model noise variance  $\sigma_w^2$  by using the variance of the DFT image model noise. Recalling the equation (52), we get

$$\hat{\sigma}_w^2 = \frac{1}{N} \sum_{j=0}^{N-1} |f_0(W_N^j)|^2 (\sigma_{\xi_r}^2(j) + \sigma_{\xi_i}^2(j)) \quad (58)$$

1-D AR model parameters of the DFT image preserve all the information which is sufficient to identify 2-D causal and semicausal AR model parameters of the original image. The identification algorithm for the other AR models is similar to the method described above.

## 4.6 Summary

The image identification and restoration algorithm we present in this chapter may be visualized by Figure 3. The input is the noisy  $N \times N$  image whose properties are not known *a priori* except for the Gaussian assumptions on the observation noise. Then, the observed image is decomposed into  $N$  1-D complex scalar subsystems, (or euivalently,  $2N$  real scalar subsystems) by using discrete Fourier transform (DFT). Applying the EM algorithm to each of the subsystems, we restore and identify the DFT image. Then, taking the inverse DFT of the restored DFT image, we get the restored  $N \times N$  original image. The AR parameters of the original image are identified from the AR parameters of the DFT image by using the least squares method.

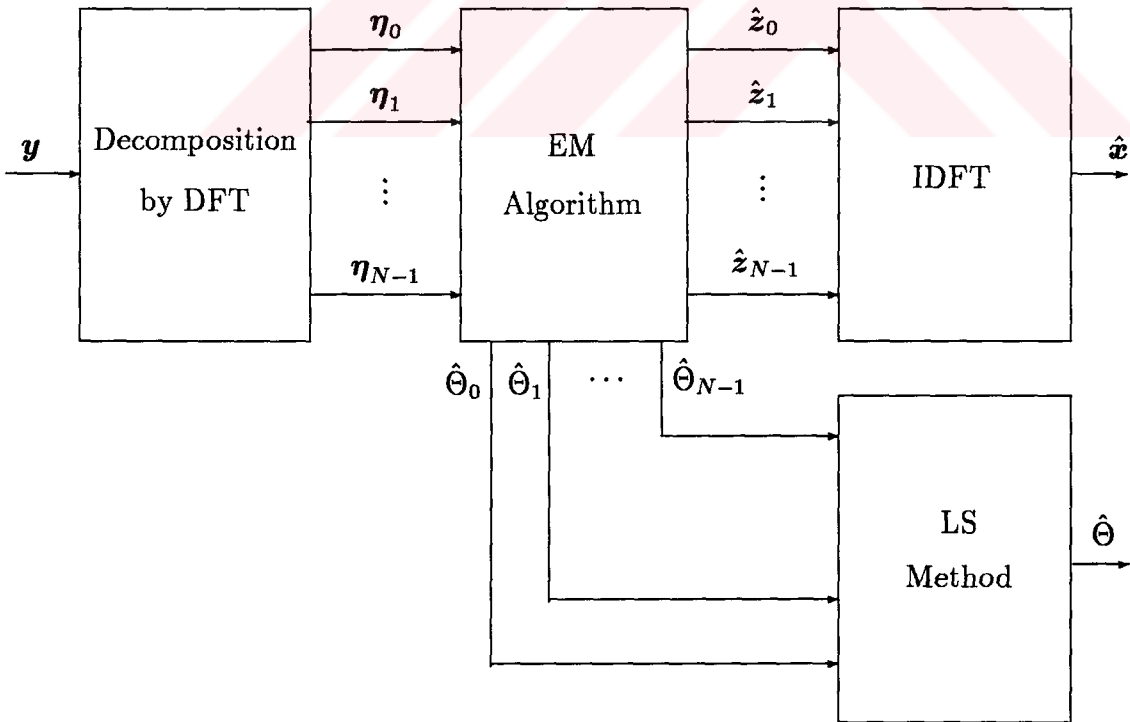


Figure 3: Schematic representation of the identification and restoration algorithm

## 4.7 Experimental Results

In this section, we present the simulation results of our identification and restoration algorithm. Experimental experience shows that the selection of the initial parameters  $\Theta$  is critical since the EM algorithm may converge to a local optimum rather than the global optimum of the likelihood function. Therefore, we should run the algorithm several times so that we can learn about the image and set the initial parameters to reasonable values for an accurate identification and restoration.

We measure the performance of image restoration by the signal to noise ratio (SNR)  $\rho$  which is defined as

$$\rho = 10 \log \frac{\sigma_x^2}{\sigma_v^2} \quad (\text{dB}) \quad (59)$$

where  $\sigma_x^2$  is the variance of the original image and  $\sigma_v^2$  is the mean squared error between the original image and the observed or restored image.

We have used the monochromatic  $100 \times 100$  face image shown in Figure 4 as the original image. Before processing, we have normalized the observed image, i.e., we have corrected for its mean value in order to satisfy the zero mean assumption on the model noise.

In Table 1 and Table 2, we present the simulation results of restoration in DFT and DST domain using Kalman filtering and maximum likelihood approach under 0 dB, 5 dB and 10 dB noise. The results presented correspond to SNR of the restored images which are displayed in Figures 6 - 19. We note the success of the restoration, especially in 0 dB noise. While the features of the face are almost lost in the noisy image, in the restored images they become extractable for the

human eye. However, the improvement in SNR decreases as the level of the noise decreases.

We measure the performance of image identification by comparing the identified parameters with the 'true' coefficients which we have found by the least squares method described in Section 2.2.1, using the noiseless original image. However, since for semicausal models, model fitting does not necessarily yield white noise driven models, we have found the true coefficients of this model in DFT domain by using the method presented in Section 4.5. Table 3 displays the AR coefficients identified in DFT domain for quarter plane, NSHP and symmetric semicausal AR models under 0 dB, 5 dB and 10 dB noise <sup>6</sup>. We observe that even at 0 dB noise the estimated parameters are very close to the true parameters. Table 4 shows the results of identification by DST for the symmetric semicausal AR model, since identification by DST is applicable to identify only this type of AR parameters. We observe that, for this model, the results of identification in DFT domain seem to be better than those in DST domain.

---

<sup>6</sup>In finding the true parameters, we have also used the constraint  $\sum_{k,l \in S} a(k,l) = 1$ , which is generally true for homogenous images as also verified by the true values of the parameters.

	<i>Kalman F.</i>	<i>Max-Like</i>
$\rho$ , 0 dB	9.6 dB	9.2 dB
$\rho$ , 5 dB	11.9 dB	11.8 dB
$\rho$ , 10 dB	14.5 dB	14.7 dB

Table 1: Performance of restoration in DFT domain

	<i>Kalman F.</i>	<i>Max-Like</i>
$\rho$ , 0 dB	9.9 dB	9.9 dB
$\rho$ , 5 dB	12 dB	12.3 dB
$\rho$ , 10 dB	15 dB	15 dB

Table 2: Performance of restoration in DST domain

	<i>Quarter plane</i>	NSHP	Semicausal
<i>True</i>	-0.45 0.77 0.67	-0.39 0.47 0.17 0.75	-0.13 0.29 0.68 -0.13 0.29
0 dB	-0.56 0.78 0.78	-0.39 0.56 0.05 0.78	-0.23 0.34 0.68 -0.23 0.34
5 dB	-0.52 0.81 0.71	-0.30 0.51 0.07 0.72	-0.19 0.34 0.70 -0.19 0.34
10 dB	-0.48 0.78 0.70	-0.22 0.42 0.08 0.72	-0.13 0.27 0.72 -0.13 0.27

Table 3: The results of identification by DFT

	0 dB	5 dB	10 dB
<i>Semi</i>	-0.35 0.47	-0.28 0.40	-0.13 0.28
<i>causal</i>	0.76	0.76	0.70
	-0.35 0.47	-0.28 0.40	-0.13 0.28

Table 4: The results of identification by DST





Figure 4: The original face image



Figure 5: 0 dB noisy image

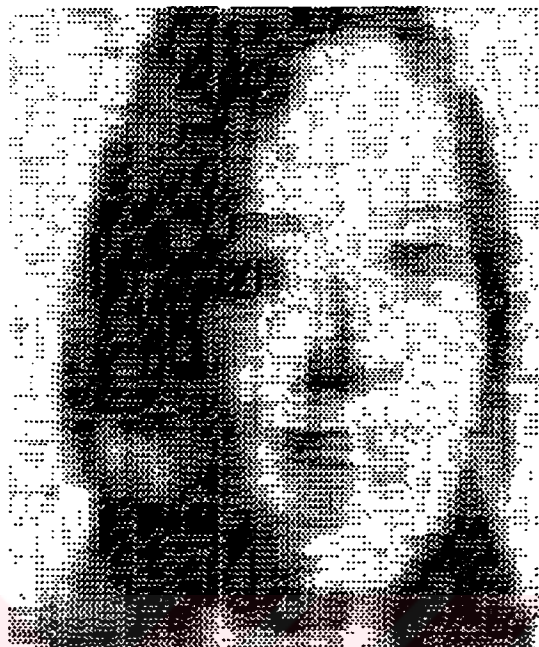


Figure 6: The image restored in DFT domain against 0 dB noise by Kalman filtering.

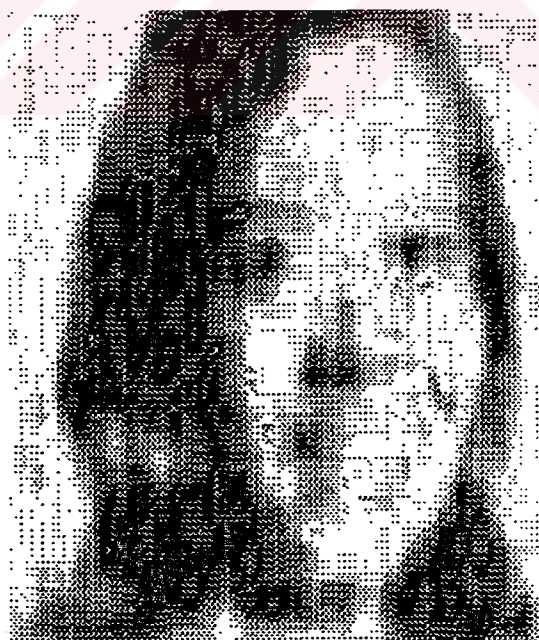


Figure 7: The image restored in DST domain against 0 dB noise by Kalman filtering

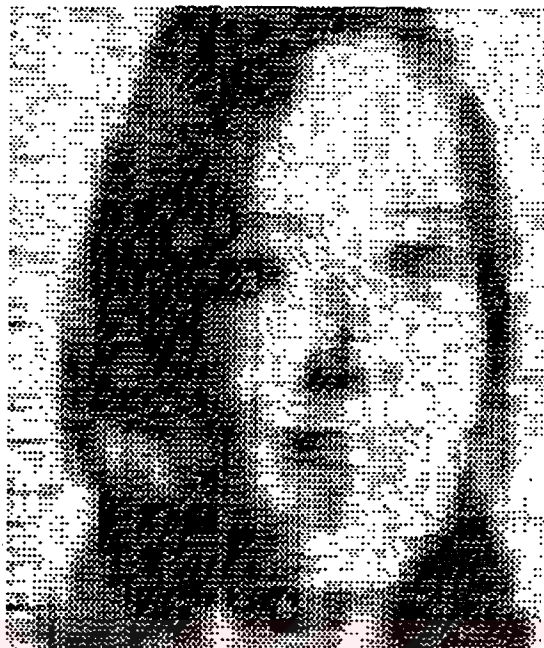


Figure 8: The image restored in DFT domain against 0 dB noise by maximum likelihood approach.

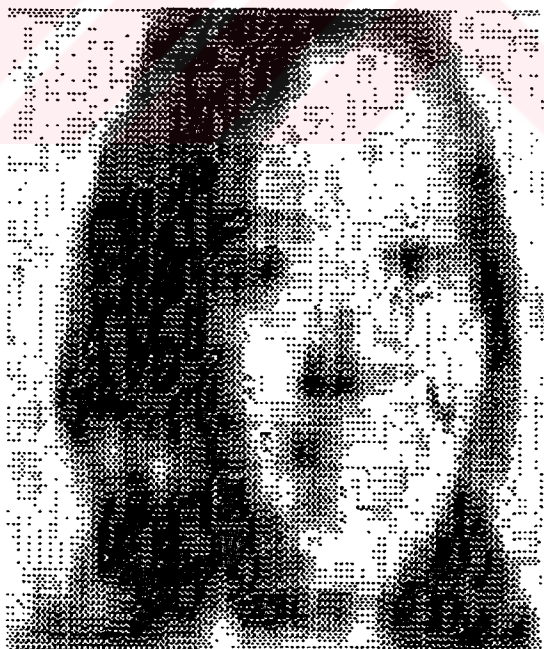


Figure 9: The image restored in DST domain against 0 dB noise by maximum likelihood approach

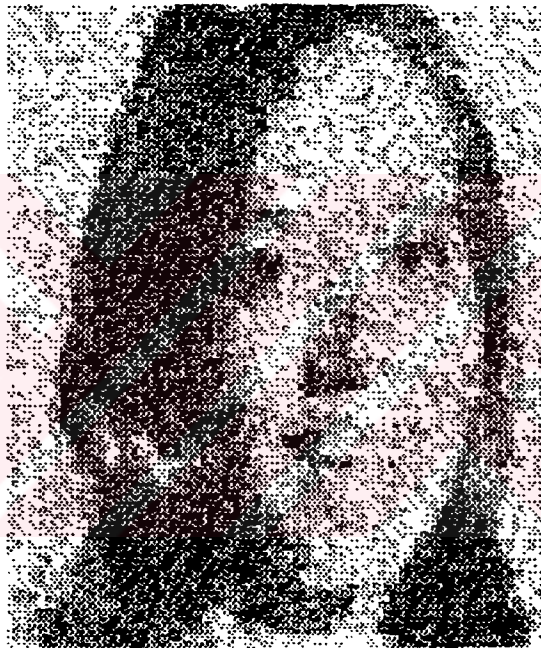


Figure 10: 5 dB noisy image

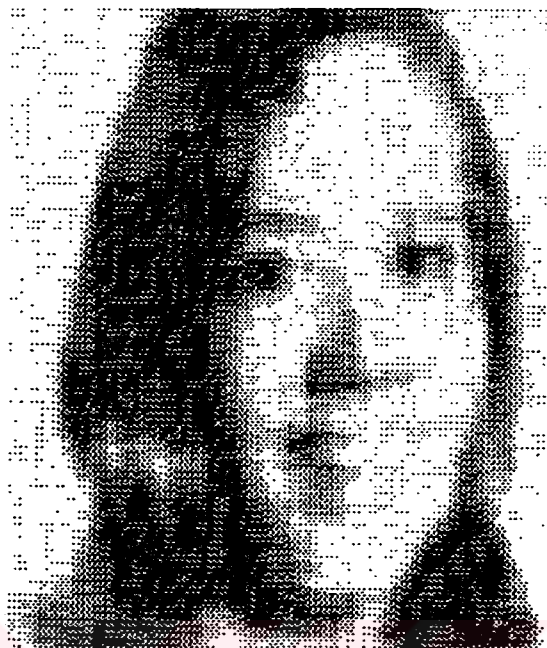


Figure 11: The image restored in DFT domain against 5 dB noise by Kalman filtering.

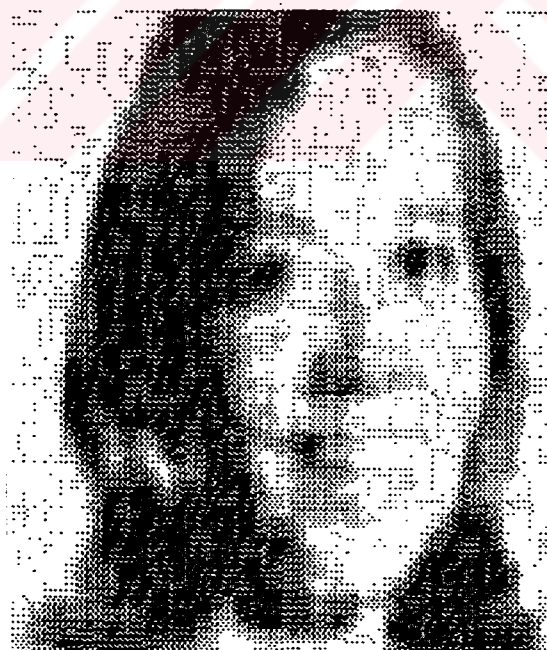


Figure 12: The image restored in DST domain against 5 dB noise by Kalman filtering.

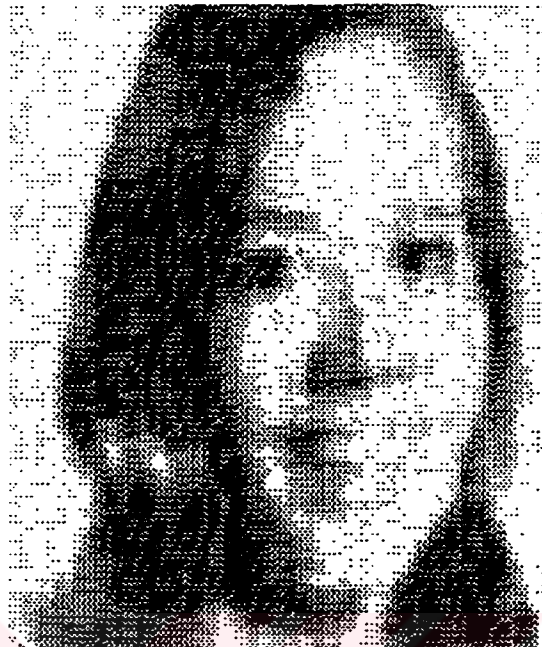


Figure 13: The image restored in DFT domain against 5 dB noise by maximum likelihood approach.

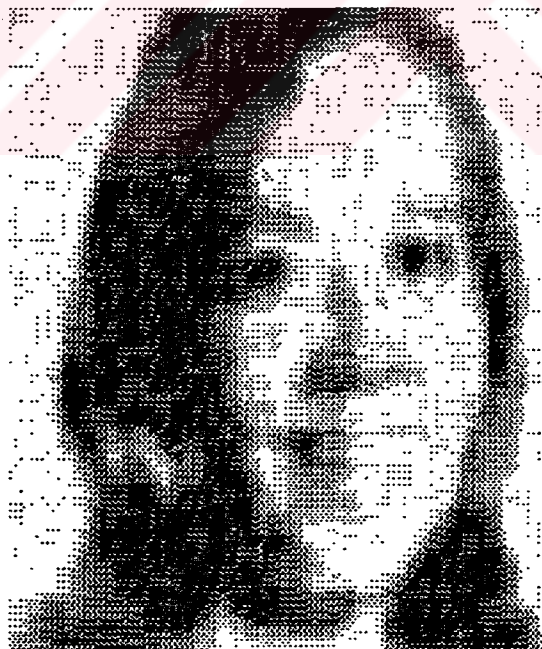


Figure 14: The image restored in DST domain against 5 dB noise by maximum likelihood approach.

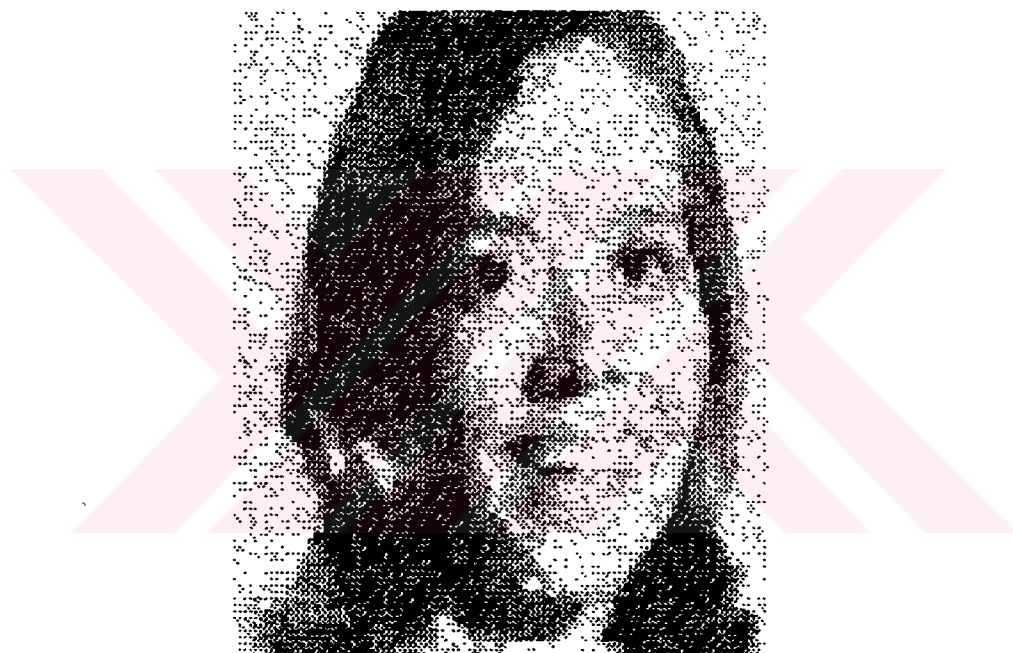


Figure 15: 10 dB noisy image

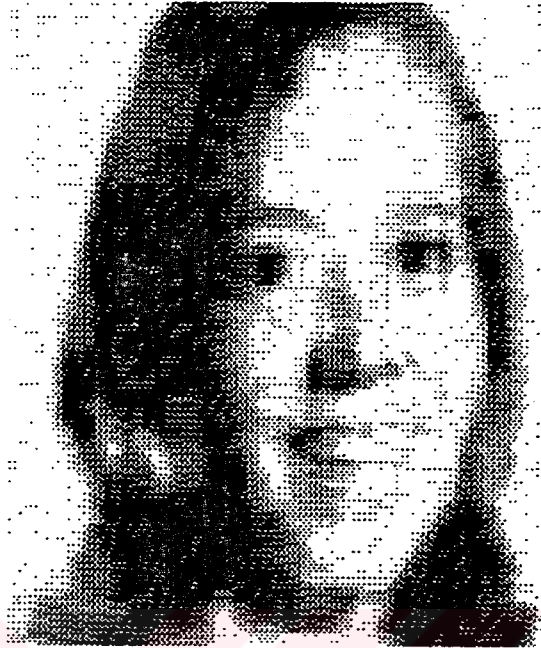


Figure 16: The image restored in DFT domain against 10 dB noise by Kalman filtering.

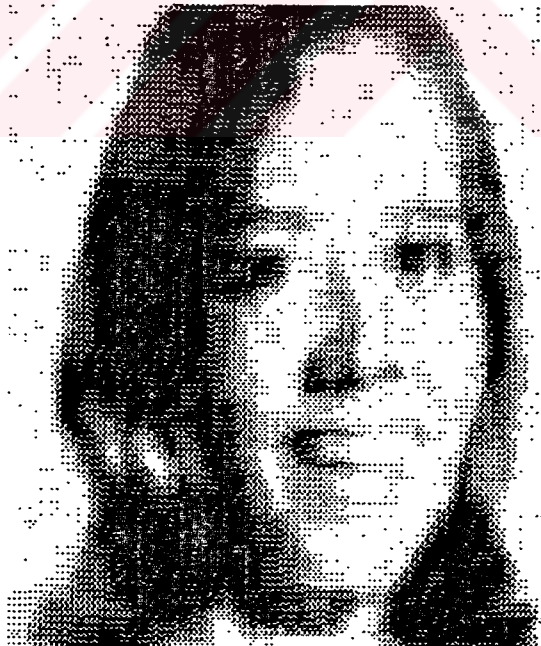


Figure 17: The image restored in DST domain against 10 dB noise by Kalman filtering



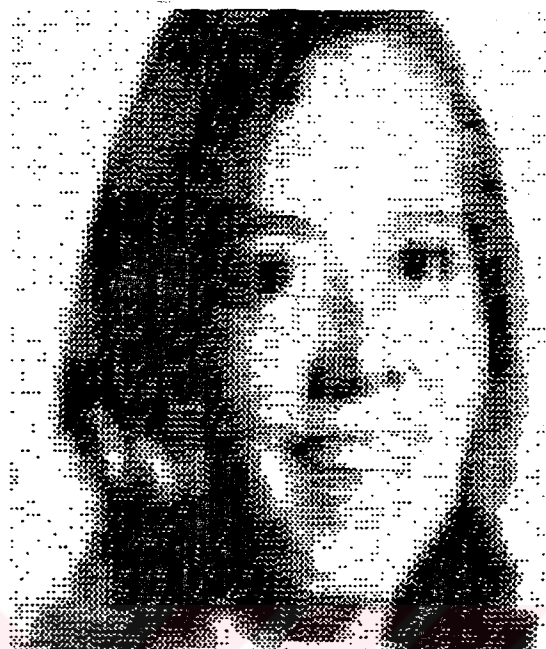


Figure 18: The image restored in DFT domain against 10 dB noise by maximum likelihood approach.

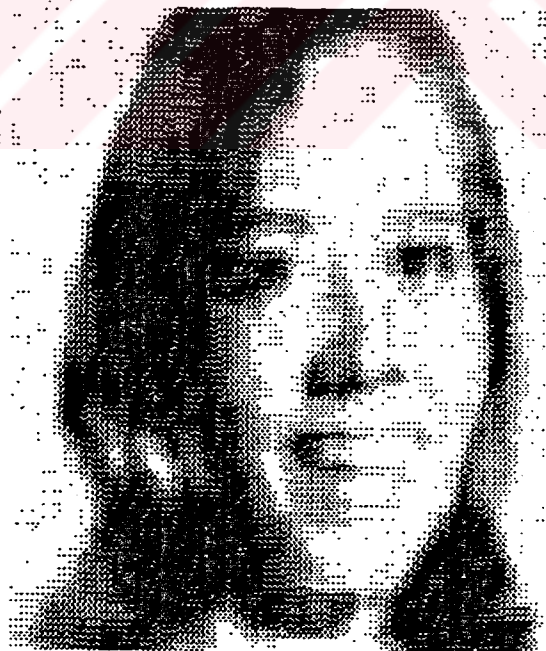


Figure 19: The image restored in DST domain against 10 dB noise by maximum likelihood approach.

## 4.8 Discussion

In this section, we will discuss the experimental results presented in the previous section.

The most important advantage of the use of DFT in our algorithm is that the 1-D AR parameters of the DFT image carry the sufficient information to identify the parameters of various types of 2-D AR models while the identification in DST domain supplies the information to identify only 2-D symmetric semicausal AR model.

The fact that, in view of the results in Table 1 and Table 2, restoration in DST domain seems slightly better than restoration in DFT domain does not have much significance since the restoration performance measure  $\rho$ , which is the only performance measure available for image restoration, is unfortunately not very accurate and reliable. For instance, if we carefully compare Figures 6 and 7, we observe that some important features of the original face image like the mouth, the nose or the eyebrows seem to be restored more successfully in DFT domain as compared to those in DST domain. Moreover, we see that there are some spurious noise in Figure 7 while the restored image in Figure 6 is smooth. We also note that identification by DFT have yield better results as seen in Table 3 and 4. Therefore, we should expect that restoration in DFT domain should be more accurate. Another reason why we expect that the results of restoration in DFT domain should be better is the approximation which is made in writing the covariance matrix of the 2-D symmetric semicausal AR model noise in Equation 19. By this approximation it has become possible to decompose the original image into scalar subsystems. What we know for symmetric semicausal modelling is that the resulting model

noise is not white. However, we do not know exactly the structure of its covariance matrix. On the other hand, since the resulting model noise is white for causal models (the use of causal models is possible if we use DFT), the assumption that the decomposed scalar subsystems are uncorrelated becomes more valid by the use of DFT. Moreover, since the selection of the initial parameters for the EM algorithm is critical, with different initial values, it is possible to end up with different results. Therefore, evaluation of our experimental results for restoration is not very straightforward. Finally, it is possible to make the conclusion that restoration in DST and DFT domain have almost equal performances. If we use the classical performance measure defined in (59), restoration in DST is slightly better. On the other hand, visually, restoration in DFT domain seems to be better.

In Table 1 and Table 2, we also compare the performances of maximum likelihood restoration and Kalman filtering. The maximum likelihood approach requires a bulk restoration process (i.e., it makes use of all the image pixels in order to restore a single pixel. ) and seems to yield better results when compared to *recursive* Kalman filtering. However, our simulation results have shown that Kalman filtering followed by a *backward smoother* yields almost equal performance as compared to the maximum likelihood restoration and is, moreover, computationally much more efficient.

## 4.9 Comments on Further Research

In this thesis, we have dealt with the restoration and identification of images degraded by Gaussian additive white noise. We have excluded another type of degradation which is called blur. However, blurring is an important problem which is usually inevitable in image identification and restoration applications.

In image processing, blurring is modelled by a 2-D point spread function (PSF) and in the existence of blur, the observation model in (1) becomes

$$y(n, m) = \sum_{k, l \in S_d} d(k, l)x(n - k, m - l) + v(n, m) \quad (60)$$

where  $d(k, l)$  is the point spread function and  $S_d$  denotes its support.

The compact form of (60) can be written in matrix form as

$$\mathbf{y} = \mathbf{D}\mathbf{x} + \mathbf{v} \quad (61)$$

where  $\mathbf{D}$  is a block circulant matrix determined by the point spread function coefficients  $d(k, l)$ .

We observe that (60) and (61) are in similar forms with the AR modelling equations (2) and (3).

In the existence of blur, image identification includes also the identification of the point spread function and image restoration must be performed also against blur. In AR modelling, the choice of the support depends on the application. However, since blur is a real phenomenon, the support is not a matter of choice any more for blur models. Therefore, the flexibility of DFT restoration and identification for different types of supports gains much more importance in the existence of blur.

In view of the observation model equations (60) and (61), if we proceed further, we end up with similar circulant blur coefficient matrices as in (16). The structure of these coefficient matrices depends on the existent blur. Therefore, reduction of dimensionality is not generally possible by using DST. On the other hand, since DFT diagonalizes any circulant matrix, we can modify our algorithm also for restoration and identification against blur. However, we need a formal derivation and this may be the subject of a further research.



## V CONCLUSION

In this thesis, we have studied the problem of image identification and restoration using the EM algorithm. By the use of the EM algorithm, we have shown that image identification and restoration are possible at the same time without *a priori* knowledge of the observation noise and the original image.

Throughout the study, we have concentrated on the reduction of dimensionality since 2-D processing of images generally yields more complex algorithms when compared to 1-D signal processing. We have presented an algorithm which reduces the 2-D problem to a 1-D problem and then identifies and restores the image by using the EM algorithm. The algorithm presented may be regarded as a modification to the method developed by Katayama [3]. However, our algorithm is superior to this method since by the use of DFT, it is capable to identify any type of 2-D AR parameters while the latter can identify only the symmetric semicausal AR model parameters. Moreover, our algorithm is promising for image identification and restoration in the existence of blur since it is flexible about the support of the blur and AR models. We have simulated the method and identified the parameters of quarter plane, NSHP and symmetric semicausal AR models successfully under noisy conditions. The performance of restoration has been almost equal with the method in [3]. However, visually, restoration in DFT domain seemed to be better.

In this thesis, we have also compared the performances of maximum likelihood restoration and Kalman filtering followed by *backward smoothing*. Since we have reduced the dimension of the processing, 1-D Kalman filtering has become possible, which is much more efficient than 2-D Kalman filtering. We have also used the maximum likelihood restoration approach more efficiently, again because

of the reduction in dimension. Experimental results have shown that these two approaches have almost equal performances. Since 1-D Kalman filtering is computationally much more efficient, in one dimension, Kalman filtering followed by backward smoothing is preferable to the maximum likelihood restoration.



## APPENDIX A

### Derivation of the Equation 28

We rewrite (16) as

$$\mathbf{x}(m) = \mathbf{A}_0^{-1} \mathbf{A}_1 \mathbf{x}(m-1) + \mathbf{A}_0^{-1} \mathbf{w}(m) \quad (62)$$

Taking the DFT of (62) yields

$$\mathbf{F}\mathbf{x}(m) = \mathbf{F}\mathbf{A}_0^{-1} \mathbf{A}_1 \mathbf{x}(m-1) + \mathbf{F}\mathbf{A}_0^{-1} \mathbf{w}(m)$$

Since  $(\mathbf{F}\mathbf{F}^* = \mathbf{I})$ , it follows

$$\begin{aligned} \mathbf{F}\mathbf{x}(m) &= \mathbf{F}\mathbf{A}_0^{-1} \mathbf{F}^* \mathbf{F} \mathbf{A}_1 \mathbf{F}^* \mathbf{F}\mathbf{x}(m-1) + \mathbf{F}\mathbf{A}_0^{-1} \mathbf{w}(m) \\ &= \mathbf{\Lambda}_0^{-1} \mathbf{\Lambda}_1 \mathbf{F}\mathbf{x}(m-1) + \mathbf{F}\mathbf{A}_0^{-1} \mathbf{w}(m) \end{aligned}$$

where

$$\begin{aligned} \mathbf{\Lambda}_0^{-1} &= \text{diag}(f_0^{-1}(W_N^0), \dots, f_0^{-1}(W_N^{N-1})) \\ \mathbf{\Lambda}_1 &= \text{diag}(f_1(W_N^0), \dots, f_1(W_N^{N-1})) \end{aligned}$$

Finally, we end up with the equation (28),

$$\mathbf{F}\mathbf{x}(m) = \mathbf{\Lambda}\mathbf{F}\mathbf{x}(m-1) + \mathbf{F}\mathbf{A}_0^{-1} \mathbf{w}(m)$$



## APPENDIX B

### Derivation of the Equations 32 and 33

By the definition (25),

$$\boldsymbol{\xi}(m) = \mathbf{F} \boldsymbol{\Lambda}_0^{-1} \mathbf{w}(m)$$

Using ( $\mathbf{F} \mathbf{F}^* = \mathbf{I}$ ) we write,

$$\begin{aligned} \boldsymbol{\xi}(m) &= \mathbf{F} \boldsymbol{\Lambda}_0^{-1} \mathbf{F}^* \mathbf{F} \mathbf{w}(m) \\ &= \boldsymbol{\Lambda}_0^{-1} \mathbf{F} \mathbf{w}(m) \end{aligned} \tag{63}$$

The covariance of  $\boldsymbol{\xi}(m)$  is defined by

$$\text{Cov}[\boldsymbol{\xi}(m)] = \text{E}[\boldsymbol{\xi}(m) \boldsymbol{\xi}^{*t}(m)] \tag{64}$$

Using (63), we write

$$\begin{aligned} \boldsymbol{\xi}(m) \boldsymbol{\xi}^{*t}(m) &= \boldsymbol{\Lambda}_0^{-1} \mathbf{F} \mathbf{w}(m) (\boldsymbol{\Lambda}_0^{-1*} \mathbf{F}^* \mathbf{w}(m))^t \\ &= \boldsymbol{\Lambda}_0^{-1} \mathbf{F} \mathbf{w}(m) \mathbf{w}^t(m) \mathbf{F}^* \boldsymbol{\Lambda}_0^{-1*} \end{aligned}$$

Then, by (18), the equation (64) becomes

$$\begin{aligned} \text{E}[\boldsymbol{\xi}(m) \boldsymbol{\xi}^{*t}(m)] &= \sigma_w^2 \boldsymbol{\Lambda}_0^{-1} \mathbf{F} \mathbf{F}^* \boldsymbol{\Lambda}_0^{-1*} \\ &= \sigma_w^2 \boldsymbol{\Lambda}_0^{-1} \boldsymbol{\Lambda}_0^{-1*} \end{aligned} \tag{65}$$

$$\tag{66}$$

where  $\boldsymbol{\Lambda}_0^{-1} \boldsymbol{\Lambda}_0^{-1*}$  is a diagonal matrix with real entries.

(65) implies the equation (32) and means  $\xi_j(m)$  and  $\xi_l(m)$  are uncorrelated for  $l \neq j$ .

The derivation of (33) is very similar to that of (32).



## APPENDIX C

### Derivation of Equation 39

Recalling (35) and (37), the complex coefficient  $a = a_r + ia_i$  is found so as to minimize the log-likelihood function (omitting the constant terms) :

$$\begin{aligned} \log p(\mathbf{z} | \Theta) &= \frac{1}{\sigma_\xi^2} \sum_{m=1}^N |z(m) - az(m-1)|^2 \\ &= \frac{1}{\sigma_\xi^2} \sum_{m=1}^N \left( z_r(m) - a_r z_r(m-1) + a_i z_i(m-1) \right)^2 \\ &\quad + \sum_{m=1}^N \left( z_i(m) - a_i z_r(m-1) - a_r z_i(m-1) \right)^2 \end{aligned}$$

where  $\sigma_\xi^2 = \sigma_{\xi_r}^2 + \sigma_{\xi_i}^2$  by (51), with respect to  $a_r$  and  $a_i$ . Differentiating the log-likelihood function with respect to  $a_i$  and setting to zero yield

$$\sum_{m=1}^N z_r(m) z_i(m-1) - z_i(m) z_r(m-1) + a_i \left( z_i^2(m-1) + z_r^2(m-1) \right) = 0$$

It follows

$$a_i = \frac{\sum_{m=1}^N z_r(m) z_i(m-1) - z_i(m) z_r(m-1)}{\sum_{m=1}^N z_i^2(m-1) + z_r^2(m-1)}$$

Since

$$\begin{aligned} \frac{1}{N} \sum_{m=1}^N z_r(m) z_i(m-1) - z_i(m) z_r(m-1) &= E[z_i(m)] E[z_r(m-1)] - E[z_r(m)] E[z_i(m-1)] \\ &= 0 \end{aligned}$$

we get the equation (39):

$$a_i = 0$$

## BIBLIOGRAPHY

- [1] A.K. Jain, "Advances in mathematical models for image processing", Proc. IEEE, Vol. 69, No. 5, pp. 502-528, 1981.
- [2] R.L. Lagendijk, Iterative identification and restoration of images, Ph.D. Thesis Delft University of Technology, 1990.
- [3] T. Katayama and T. Hirai, "Parameter identification for noisy image via the EM algorithm", Signal Process., Vol. 20, No. 1, pp. 15-24, May 1990.
- [4] J.W. Woods and C.H. Radewan, "Kalman filtering in two-dimensions", IEEE Trans. Information Theory, Vol. 23, No. 4, pp. 473-482, 1977.
- [5] H. Kaufman, J.W. Woods, S. Dravida and A.M. Tekalp, "Estimation and identification of two-dimensional images", IEEE Trans. Autom. Control, Vol. 28, No. 7, 1983.
- [6] M.P. Ekstrom and J.W. Woods, "Two-dimensional spectral factorization with applications in recursive digital filtering", IEEE Trans. ASSP., Vol. 24, No. 2, pp. 115-128, 1976.
- [7] A.K. Jain, Fundamentals of Digital Image Processing, Prentice Hall, Englewood Cliffs NJ, 1989.
- [8] R.L. Lagendijk, J. Biemond and D.E. Boeke, "Regularized iterative image restoration with ringing reduction", IEEE Trans. ASSP., Vol. 36, No. 12, pp. 1874-1888, 1988.

- [9] R.W. Schafer, R.M. Mersereau and M.A. Richards, "Constrained iterative signal restoration algorithms", Proc. IEEE, Vol. 69, No. 4, pp. 4322-450, 1981.
- [10] J.W. Woods and V.K. Ingle, "Kalman filtering in two-dimensions: Further results", IEEE Trans. ASSP., Vol. 29, No. 2, 1981.
- [11] B.R. Musicus and J.S. Lim, "Maximum likelihood parameter estimation of noisy data", Proc. 1979 IEEE Int. Conf. ASSP., pp. 224-227.
- [12] M. Feder and E. Weinstein, "Parameter estimation of superimposed signals using the EM algorithm", IEEE Trans. ASSP., Vol. 36, No. 4, pp. 95-103, 1988.
- [13] A.P. Dempster, N.M. Laird and D.B. Rubin, "Maximum likelihood from incomplete data", J. Royal Statist. Soc. B, Vol. 39, pp. 1-38, 1977.
- [14] A.K. Jain and E. Angel, "Image restoration, modelling and reduction of dimensionality", IEEE Trans. Comp., Vol. 23, No. 5, pp. 470-476, 1974.
- [15] A.K. Jain, "An operator factorization method for restoration of blurred images", IEEE Trans. Comp., Vol. 26, No. 11, pp. 1061-71, 1977.
- [16] W.B. Davenport, Probability and Random Processes, McGraw-Hill, Inc. , 1970.
- [17] J.S. Meditch, Stochastic Optimal Linear Estimation and Control, McGraw-Hill, Inc. , 1969.
- [18] M. Tanaka and T. Katayama, "Edge detection and restoration of noisy images by the expectation-maximization algorithm", Signal Process., Vol. 17, pp. 213-226, 1989.